Applied Surface Science 508 (2020) 145254

Contents lists available at ScienceDirect

Applied Surface Science

journal homepage: www.elsevier.com/locate/apsusc

Full Length Article

Effect of internal stress on short-circuit diffusion in thin films and nanolaminates: Application to Cu/W nano-multilayers

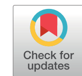

Aleksandr V. Druzhinin[a,b,c,*], Bastian Rheingans[a], Sebastian Siol[a], Boris B. Straumal[b,c,d], Jolanta Janczak-Rusch[a], Lars P.H. Jeurgens[a], Claudia Cancellieri[a,*]

[a] Empa, Swiss Federal Laboratories for Materials Science and Technology, Laboratory for Joining Technologies and Corrosion, Überlandstrasse 129, Dübendorf CH-8600, Switzerland

[b] National University of Science and Technology «MISIS», Leninsky Prospect 4, Moscow 119049, Russian Federation

[c] Institute of Solid State Physics and Chernogolovka Scientific Center, Russian Academy of Sciences, Moscow District, Academician Ossipyan Str., Chernogolovka 142432, Russian Federation

[d] Karlsruhe Institute of Technology (KIT), Institute of Nanotechnology, Hermann-von-Helmholtz-Platz 1, Eggenstein-Leopoldshafen 76344, Germany

ARTICLE INFO

Keywords:
Grain boundary diffusion
Internal stress
Auger electron spectroscopy
Nano-multilayers
Hwang–Balluffi model

ABSTRACT

The stability, reactivity and functionality of modern nanostructured and nanoarchitectured materials, like nano-multilayers (NMLs) and nanocomposites (NCs), are generally ruled by fast short-circuit diffusion of atoms along internal interfaces, such as phase and grain boundaries (GBs), at relatively low temperatures. Residual stresses can have a significant effect on the kinetics of short-circuit diffusion in these nanomaterials, which has been largely neglected up to date. We present a combined experimental-modelling approach for deriving stress-free activation energies (and related diffusion coefficients) for the grain boundary diffusion of a given element across an inert barrier nanolayer, which can be utilized to perform fundamental investigations and model predictions of GB diffusion kinetics across inert barrier nanolayers in the presence of a varying stress field. The method was applied to investigate the diffusion of Cu along W grain boundaries in Cu/W nano-multilayers in the temperature range from 400 °C to 600 °C. Firstly, the GB diffusion kinetics as function of the temperature and stress state were determined from experiment by combining *in situ* heating AES analysis and *ex situ* XRD stress analysis. The experimental data were compared to model predictions from a modified Hwang–Balluffi model, which accounts for a varying stress level within the barrier during the annealing. The extracted stress-free activation energy for grain boundary diffusion of Cu in W (~0.29 eV) is substantially lower than the respective experimental value for a high compressive stress within the W barrier nanolayer. The corresponding stress-free Cu GB diffusion coefficient in W equals $D_b^* = (3.2 \pm 0.6) \times 10^{-15} \exp(-0.29 \pm 0.02 \mathrm{eV/kT})\ \ \mathrm{cm^2/s}$.

1. Introduction

Grain boundary (GB) diffusion plays a major role in the engineering of nanocrystalline materials [1]. In low-dimensional materials with an ultrafine grain structure, e.g. thin nanograined films or nano-multilayers (NMLs), the thermal stability of the microstructure and its evolution upon low-temperature thermal treatment are predominantly governed by the atom diffusion fluxes along internal interfaces, e.g. grain boundaries and phase boundaries, acting as short-circuit paths for fast atom transport [2,3]. Only at relatively high temperatures with respect to the bulk melting temperature (i.e. for $T > 0.7T_m$, where T_m denotes the melting temperature of the solid), volume (lattice) interdiffusion can become dominant and result in Kirkendall porosity and/or the formation of interfacial reaction layers [4,5]. Control of the diffusion fluxes along the GBs and internal interfaces at relatively low temperatures ($T < 0.5T_m$) provides a tool for designing the microstructure and integrity down to the nanoscale [6–8] and thereby for tailoring the properties of functional nanomaterials and nanoarchitectures. For instance, controlling the grain boundary diffusion kinetics is crucial for the performance of thin film diffusion barriers of interconnects in microelectronic devices [9,10]: doping through GB diffusion can occur, which alters the electronic and thermal conductivity [11]. Furthermore, atomically sharp interfaces are essential for NMLs used for x-ray and neutron mirrors, as well as for spintronic applications: for such NML applications, grain boundary diffusion along triple junctions can play a major role in the sharpening of interfaces [12]. The

* Corresponding authors at: Empa, Swiss Federal Laboratories for Materials Science and Technology, Laboratory for Joining Technologies and Corrosion, Überlandstrasse 129, Dübendorf CH-8600, Switzerland (C. Cancellieri and A. V. Druzhinin).

E-mail addresses: druzhininsas@mail.ru (A.V. Druzhinin), claudia.cancellieri@empa.ch (C. Cancellieri).

https://doi.org/10.1016/j.apsusc.2020.145254
Received 17 October 2019; Received in revised form 4 December 2019; Accepted 1 January 2020
Available online 03 January 2020
0169-4332/ © 2020 Elsevier B.V. All rights reserved.

performance of spin-valve multilayers can also be degraded by grain boundary diffusion [13].

Nanoscale diffusion is the main cause for thermal degradation of NMLs can also be exploited in a positive way, for example, for the fabrication of metallic nanocomposites (NCs). In the latter case, starting from a NML structure of alternating nanolayers of two immiscible metals, the high-temperature thermal degradation of the NML proceeds by diffusion-controlled thermal grooving of grain boundaries, pinching-off of the nanolayers and subsequent spheroidization of residual layer-fragments, leading to a NC architecture [14–17]. The NML-to-NC transformation provides a possibility to tune the NC microstructure (as well as e.g. the mechanical [18], thermal [19] and electrical [20] properties) by controlled variation of the relative volume fractions and sizes of the constituent phases of the initial NML [17]. A recent study on the NML-to-NC transformation in the immiscible system Cu/W [14,17] showed that GB diffusion of Cu atoms along W GBs becomes already thermally activated at low temperatures in the range of 400 °C $< T <$ 600 °C, and acts as the initial stage of the NML degradation process [17]. The initial stage of GB diffusion of Cu is postulated to proceed preferentially along high-angle W GBs in the GB network of the barrier layer, as is the case for e.g. Si diffusion within the high-angle GBs of Al layers [21]. The NML-to-NC transition then proceeds at a somewhat higher temperatures of $T \geq 700$ °C by the thermally-activated transport of W atoms along the majority of internal interfaces (e.g. phase and grain boundaries), leading to progressive degradation of the nanolayered structure.

In general, NMLs prepared by magnetron sputtering exhibit large internal residual (macro-)stresses, which have a pronounced effect on the NML-to-NC transition [14,17,22]. Cu/W NMLs were found, in particular, to exhibit considerable compressive stress in the as-deposited state due to the large interface stress originating from partially coherent Cu(1 1 1)/W(1 1 0) interfaces, which prevails over the superimposed deposition (growth) and coherency stresses [17]. The resulting stress fields at the W GBs affect the chemical potential gradient and diffusivity of Cu within the W GBs [23] and thereby the kinetics of the NML-to-NC transition during annealing. According to Ostrovsky et al. [24], stress in a diffusion barrier can substantially modify the GB diffusion (including self-diffusion): the mean stress can either accelerate or decelerate the diffusion flux in the GB through the modification of the (effective) activation energy for diffusion, while the stress gradient changes the saturation level of the diffusant concentration on the barrier layer surface. Also, Balandina et al. [25] experimentally demonstrated for the Cu/Ni system that the presence of stress gradients in a Ni diffusion barrier modifies the effective GB diffusion coefficient of Cu atoms with respect to the stress-free state. Hence, the effect of stress fields on GB diffusion needs to be accounted in the derivation of stress-free value of the activation energy and diffusion coefficient from experiment, since the stress-free value is required as an input to any model calculation.

GB diffusion in thin films is commonly studied by the surface-accumulation method [26–33]. This method is applicable for the low temperature range at which volume diffusion is kinetically frozen and mass transport in the thin film is mainly governed by GB diffusion with negligible leakage of the GB diffusing species into the adjoining grains of the chemically inert barrier (classified as Type C kinetics [34]). In this regime, the diffusing atoms (diffusant) migrate through the GBs to the free surface of the chemically inert barrier layer and accumulate there, often aided by surface diffusion [35]. In the surface-accumulation method, the GB diffusion coefficients are derived by measuring the time evolution of the average diffusant concentration on the surface of the thin film during isothermal annealing. These experiments can be well performed using *in situ* surface-sensitive analytical techniques, like *in situ* heating Auger Electron Spectroscopy (AES), for film thicknesses in the nanometer range ($\leq$10 nm). At relatively low annealing temperatures, grain coarsening and recrystallization of the barrier layer proceed only very slowly, thus largely preserving the GB microstructure during the diffusion experiment. The conventional kinetic evaluation of the surface-accumulation method, however, does not consider the internal stress in the diffusion barrier and unfortunately, up to date, only very few experimental studies on the effect of stresses on GB diffusion have been reported [25].

In the present study, *in situ* heating Auger Electron Spectroscopy analysis is applied to investigate the GB diffusion of Cu along W GBs in Cu/W NMLs, focusing on the effect of internal stresses in the W nanolayers on the GB diffusion kinetics. A diffusion model, which includes the time evolution of stress in the barrier layer during annealing, is derived and applied to extract the stress-free diffusion coefficients and activation energies for the GB diffusion of Cu in W. A fundamental understanding of the kinetics of Cu diffusion in GBs in dependence of the stress evolution during annealing is presented and related to the rate of the NML-to-NC transformation.

2. Experimental methods

Cu/W NMLs were deposited at room temperature on 10 × 10 mm^2 polished α-Al_2O_3 (0 0 0 1) single-crystalline wafer substrates (i.e. sapphire-C wafers) by magnetron sputtering in an ultrahigh vacuum chamber (base pressure $< 10^{-8}$ mbar) from two confocally arranged, unbalanced magnetrons equipped with targets of pure W (99.95%) and pure Cu (99.99%). Before insertion in the sputter chamber, the sapphire substrates were ultrasonically cleaned using acetone and ethanol. Prior to the deposition, possible surface contamination on the α-Al_2O_3 (0 0 0 1) substrate was removed by Ar^+ sputter cleaning for 5 min applying an RF Bias of 100 V at a working pressure of 1.6×10^{-2} mbar. The RF Bias was maintained during the NML deposition at a working pressure of approximately 5×10^{-3} mbar. First, a 25 nm thick W buffer layer was deposited on the sputter-cleaned substrate. Next, NMLs consisting of 20 repetitions of a Cu/W building block were deposited on top. Two NML configurations were prepared by controlled variation of the Cu and W nanolayer thicknesses of the Cu/W building block (bilayer): 10 nm Cu / 3 nm W (10Cu/3W) and 5 nm Cu / 5 nm W (5Cu/5W). Detailed cross-sectional analysis of the Cu/W NMLs before and after thermal annealing at different temperatures by High-Resolution Scanning (HR-SEM) and Transmission Electron Microscopy (HR-TEM) are reported elsewhere Refs. [14,17,22]. These studies show that the Cu/W NMLs degrade into a nanocomposite only at annealing temperatures above 800 °C (for 100 min in vacuum). Importantly, in the immiscible Cu/W system, no compound intermediate layers were observed at the evolving Cu/W interfaces during the annealing.

In situ Auger electron spectroscopy annealing was performed using a Physical Electronics PHI-4300 SAM system equipped with a cylindrical mirror analyzer (CMA; constant relative energy resolution ΔE/E of 0.3%) and a coaxial electron gun operating at 5 keV with an emission current of 50 μA. Analysis was conducted with a beam current of 30 nA, resulting in an electron beam spot of about 1 μm with an accumulation time of 20 ms/eV. Before *in situ* analysis, each sample (NML) was heated-up during 40 min to the annealing temperature, assuming that the heating-up time is sufficient for establishing a quasi-steady-state in the W GB network structure [26]. Each spectrum was recorded with 15 iterations with a total duration of around 6 min. The annealing time for each data point includes the time for recording the spectra. The Auger instrumental detection limit for most of atoms ranges between 0.01 and 0.1 at.%. In our used experimental conditions, the Cu detection limit is around 0.1–1 at.%. The thermal dose of the focused electron beam on the Cu/W NML was estimated using the models proposed by Friskney et al. [36] and Hofmann et al. [37] (using the thermal conductivity of W as the lower-bound of the thermal conductivity in the NML): the calculations indicate that the increase in sample temperature due to the e-beam irradiation does not exceed 1.5 K, which is in the range of the measurement error of the temperature and can thus be neglected. Notably, the recorded spectra from the surface of as-deposited NMLs (i.e.

before annealing) did not reveal any signal of residual Ar atoms, which might be implanted into the nanolayer during the sputter deposition process. Minor surface contaminations from adventitious carbon and oxygen, as measured in the as-deposited state before *in situ* annealing, could no longer be detected during the annealing.

The evolution of the Cu signal intensity in function of annealing time was measured by monitoring the ratio of the peak-to-peak intensities of the Cu LMM (920 eV) and W MNN (1736 eV) Auger lines. Annealing was performed at three different temperatures, 400 °C (673 K), 500 °C (773 K) and 600 °C (873 K). *In situ* monitoring of the temperature was performed using an Eurotherm regulator (919/909 model) with a Chromel-Alumel thermocouple junction fixed on the sample holder clamp. The pressure in the ultra-high vacuum chamber was maintained in the 10^{-10} mbar range during the annealing. The recorded spectra were processed in a derivative type (differentiation with 5 points, Savitzky-Golay smoothing with 5 points) using the MultiPak v6.1A program package, which included Auger sensitivity factors for the Cu LMM and W MNN Auger lines.

A Bruker D8 Discover X-ray diffractometer operating in Bragg-Brentano geometry with Cu K $\alpha_{1,2}$ radiation (including Ni filter) at 40 kV / 40 mA was used to measure the internal stress in point focus geometry. Stress analysis was carried out using the Crystallite Group Method (CGM) [38], suitable for highly textured systems (the deposited Cu/W NMLs possess a pronounced in-plane and out-of-plane texture [14,22]). Multiple reflections belonging to the Cu < 1 1 −2 > and W < 1 −2 1 > crystallite groups were selected for the stress analysis. All annealed NMLs were measured *ex situ* after cooling down to room temperature (RT). *In situ* stress measurements were carried out using a domed hot stage for four-circle goniometers (DHS 1100) in a vacuum atmosphere of 10^{-1} mbar, mounted directly on the D8 diffractometer. For the *in situ* stress measurement the $\sin^2\psi$ method was applied to the W(2 1 1) reflection [39] (see Supplementary Information, S. II). The reference strain-free bulk lattice parameters of Cu and W are $a_{cu} = 3.615$ Å [40] and $a_w = 3.165$ Å [41], respectively (taken at room *T*). The values of elastic constants used in the stress calculation are taken from Refs. [42] (for Cu) and [43] (for W).

3. Methodology

Consider the case of a thick layer with an infinite source of diffusant atoms, which is covered by a chemically inert surface barrier, as sketched in the left panel of Fig. 1. Bulk and GB diffusion of the diffusant in the barrier layer can be separated by selecting the temperature range at which these different diffusion regimes become thermally activated. According to Harrison [34], for Type C kinetics (applicable for temperatures lower than the half of the diffusion barrier melting point, i.e. for $T < 0.5T_m$), GB diffusion prevails over volume diffusion, i.e. $D_{GB} \gg D_{lattice}$. If GB diffusion prevails, the diffusant atoms (source) will diffuse through the GB network of the barrier layer to the free surface (sink), and then gradually spread out over the barrier layer surface by surface diffusion, eventually forming a several atomic layers thick segregated film (see left panel in Fig. 1). Generally, the surface diffusion coefficient is much larger than the GB diffusion coefficient $D_{surface} \gg D_{GB} \gg D_{lattice}$ [35], which prevents local accumulation of diffusant atoms on the surface.

For the above case, an approximate equation for the concentration of diffusant atoms on the barrier surface as a function of time was derived by Hwang and Balluffi [35]. In their model, a thin barrier film of thickness h with an average columnar grain width d is considered. The barrier film contains an array of parallel GBs, which are treated as rectangular slabs of uniform thickness δ with a constant diffusion coefficient D_b (all parameters are presented in the left panel of Fig. 1). A quasi-steady-state in the GB is considered, which implies that the concentration of diffusant atoms in the GB rapidly adjusts itself for every concentration change of diffusant atoms at the free surface. A linear concentration profile of diffusant atoms within the GB is assumed.

The average concentration of diffusant atoms c_s on the barrier surface as a function of time t for a uniform surface concentration is expressed by («Hwang–Balluffi model»):

$$c_s(t) = c_0\frac{k^{''}}{k^{'}}[1 - \exp(-St)], \tag{1}$$

where

$$S = \frac{\delta}{\delta_s}\frac{2D_b}{k^{''}dh} \tag{2}$$

and

$$D_b = D_0\exp\left(-\frac{E_A}{kT}\right). \tag{3}$$

The value δ_s corresponds to the thickness of the segregated atom

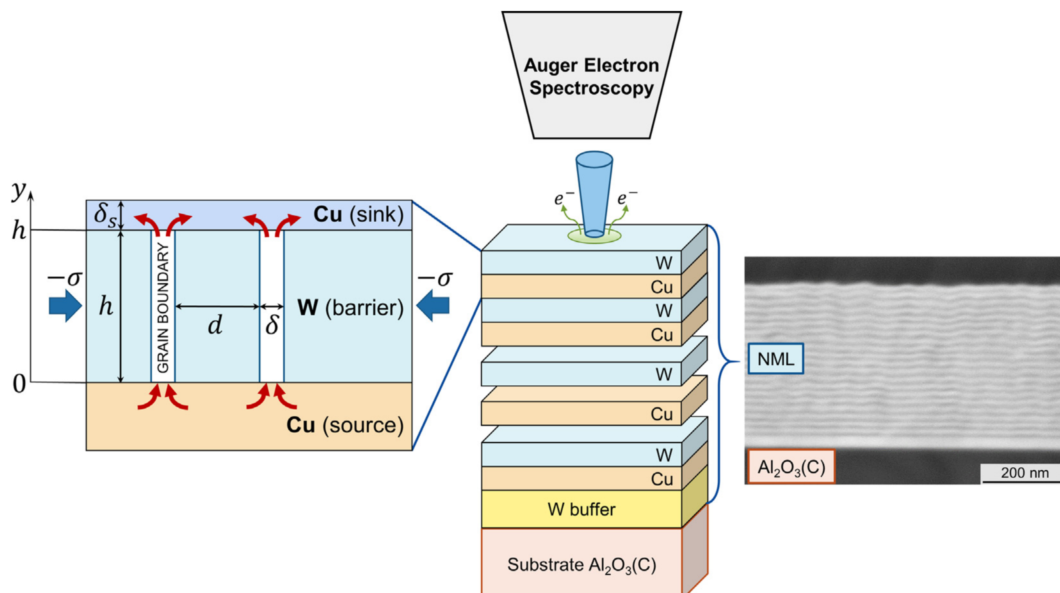

Fig. 1. Illustration of the *in situ* AES analysis of Cu diffusion in W GBs in Cu/W NMLs. Parameters used for the diffusion models are shown on the left panel. A scanning electron microscopy image of a Cu/W NML cross-section is shown on the right panel.

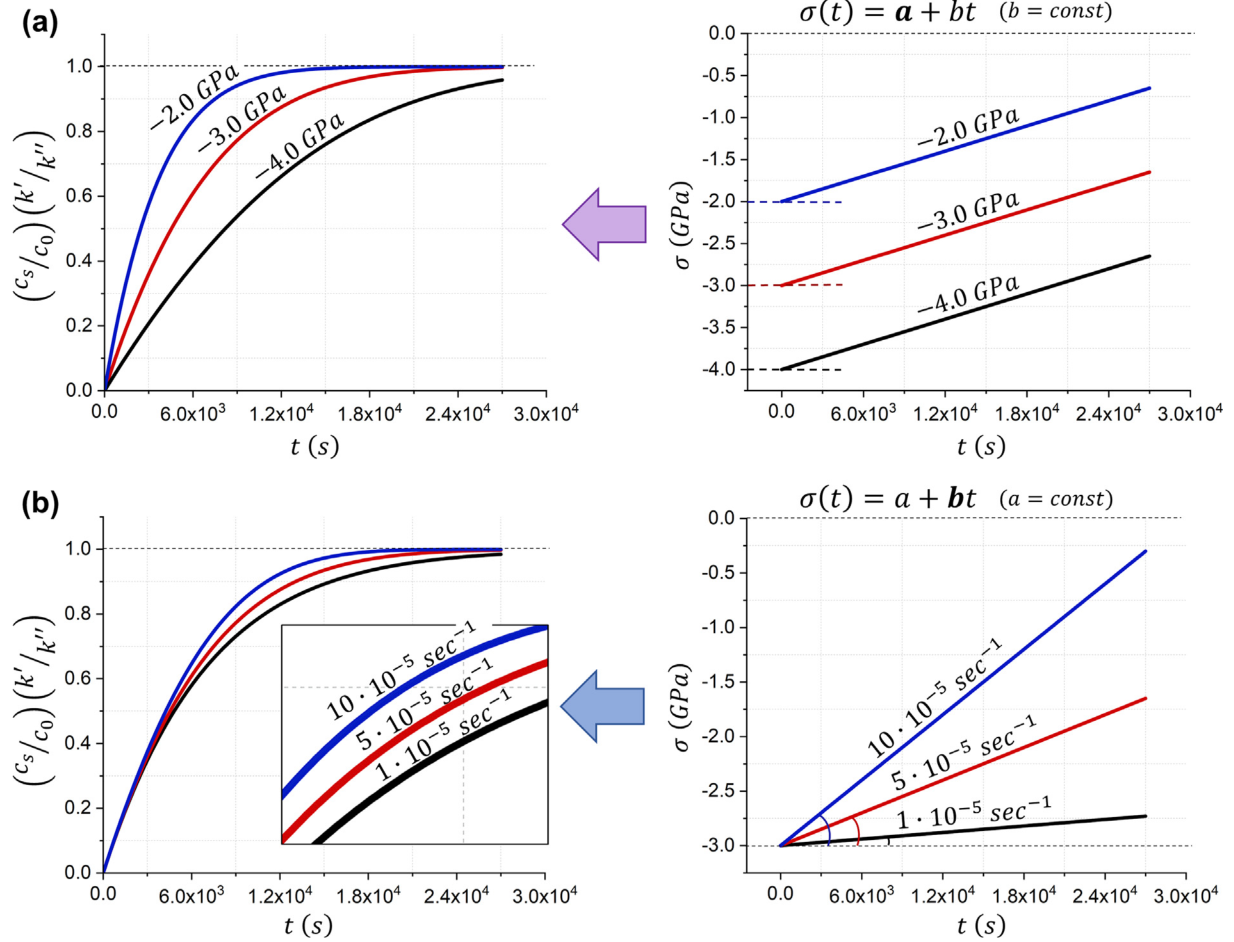

Fig. 2. Time dependence of $(c_s/c_0)(k^{'}/k'')$ calculated for different mean stress–time evolutions $\sigma_{ii}(t)$ (S = 0.001, P = 0.326 × 10^{-9}). Exemplary calculated dependence on (a) the initial (compressive) mean stress σ_0 (constant slope b = $5{\cdot}10^{-5}\,\frac{1}{s}$) and (b) the stress relaxation rate for a constant initial mean stress σ_0 = –3 GPa.

film on the accumulated surface; $2/d$ is the GB density for a barrier layer having columnar grains of width d; $k^{''} = c_{s,eq}/c_{b,eq}$ and $k^{'} = c_{0,eq}/c_{b,eq}$ are segregation coefficients, defining the local equilibria at the junction of the GB with the free surface and at the junction of the GB with the source layer, respectively (with $c_{b,eq}$ and $c_{0,eq}$ being the concentrations in the GB and in the source layer). D_0 is the pre-exponential factor of the GB diffusion coefficient and E_A the effective activation energy for GB diffusion derived by Hwang–Balluffi model; k is the Boltzmann constant. This solution is applicable if the concentration of diffusant atoms at the barrier GB/source interface remains constant with time (c_0 = const).

The effect of internal stress of the diffusion barrier on the rate of GB diffusion was comprehensively investigated by Ostrovsky et al. [23,24,44] A mean stress σ_{ii} in the barrier layer, as well as a linear stress gradient parallel to the GB plane were considered. However, for barrier layer thicknesses in the nanoscale regime, the impact of stress imposed by the source/barrier interface, the so-called interface stress [45], can prevail over all other stress contributions (e.g. growth stress, coherency stress) and thus dominate the mean stress state of the barrier layer. Interface stress can be especially significant for interfaces between materials with high lattice mismatch (i.e. forming high misfit dislocation density) as is the case for the studied Cu/W system [46]. For individual layer thicknesses in the nanoscale regime, as for the Cu/W NMLs under study, the variation of stress across the nanolayer will be considerably smaller than the mean stress value σ_{ii}, and, consequently, the stress gradient across the diffusion barrier may be neglected.

A mean stress σ_{ii} in a barrier layer modifies the activation energy term in the general expression of the GB diffusion coefficient according to [24]:

$$D_b(\sigma) = D_0 \exp\left(-\frac{E_A^* - \frac{\sigma_{ii}\Omega}{3N_A}}{kT}\right) = D_b^* \exp\left(\frac{\sigma_{ii}\Omega}{3RT}\right) \tag{4}$$

with

$$D_b^* = D_0 \exp\left(-\frac{E_A^*}{kT}\right), \tag{5}$$

where D_b^* is the GB diffusion coefficient in absence of stress (i.e. with the stress-free activation energy term E_A^*); N_A and R are the Avogadro and gas constants, respectively. $\sigma_{ii} = \sigma_{11} + \sigma_{22} + \sigma_{33}$ is the first invariant of the stress tensor; Ω is the activation volume for diffusion. Typically, polycrystalline thin films exhibit an isotropic in-plane state of stress and then $\sigma_{11} = \sigma_{22} = \sigma$, $\sigma_{33} = 0$ (the first invariant of stress tensor is $\sigma_{ii} = 2\sigma$). The presence of compressive mean stress (negative in sign) in the barrier layer results in an increase of the effective activation energy, i.e. $E_A = E_A^* + \frac{|\sigma_{ii}|\Omega}{3N_A}$, while a tensile mean stress (positive in sign) tends to a decrease it, i.e. $E_A = E_A^* - \frac{|\sigma_{ii}|\Omega}{3N_A}$.

During isothermal annealing, stresses in the barrier σ_{ii} can gradually relax due to the thermal activation of internal stress relaxation mechanisms such as creep [47] or material outflow to the surface [48], or mechanical processes such as buckling [49] or cracking [50].

Assuming that the stress relaxation with time $\sigma(t)$ occurs in-plane isotropic and follows a linear dependence, the mean stress $\sigma_{ii}(t)$ is given by:

$$\sigma_{ii}(t) = 2\sigma(t) = 2(\sigma_0 + bt), \tag{6}$$

where σ_0 is the initial stress in the barrier ($t = 0$), b is defined as the stress relaxation rate.

The modified expression for the average concentration of diffusant atoms on the barrier surface c_s as a function of time t, accounting for the stress $\sigma(t)$ in the barrier layer, can then be expressed as («Stress model»):

$$c_s(t) = c_0 \frac{k^{''}}{k^{'}} \left[1 - e^{\frac{S}{2Pb}\exp(2P\sigma_0)} e^{-\frac{S}{2Pb}\exp(2P(\sigma_0 + bt))} \right] \tag{7}$$

where

$$S = \frac{\delta}{\delta_s} \frac{2D_b^*}{k^{''}dh}, \tag{8}$$

where $P = \Omega/3RT$. In contrast to the original Hwang–Balluffi model, the factor S now includes the stress-free GB diffusion coefficient, D_b^*, pertaining to Eq. (5). The derivation of Eq. (7) is given in the Supplementary Information, P.I. If the barrier stress is constant with time ($b = 0$), a modified version of the Hwang–Balluffi model (Eq. (1)) with a constant stress contribution term can be derived (see Eq. S6 in Supplementary Information, P.I.). Stress-free GB diffusion coefficients with their respective stress-free activation energy E_A^* (at a given temperature) can be obtained by fitting $c_s(t)$ to the respective experimental data, while incorporating the experimentally determined time-dependent stress evolution $\sigma_{ii}(t)$.

A parameter study was performed on the basis of Eq. (7) to investigate the course of the surface diffusant concentration (normalized by a factor of $c_0 \frac{k^{''}}{k^{'}}$) at different temperatures and for different stress evolutions $\sigma_{ii}(t)$ (Fig. 2). It follows that the kinetics of the surface concentration evolution significantly depends on the compressive stresses in the barrier: for higher compressive barrier stresses, saturation of the surface diffusant concentration is reached only after longer annealing times (Fig. 1(a)). Even pronounced relaxation of the compressive barrier stresses during annealing (corresponding to the slope of $\sigma_{ii}(t)$ in the right panel of Fig. 2(b)) still considerably decelerates the GB diffusion rate.

In practice, the course of the average diffusant surface concentration c_s during annealing can be easily measured by *in situ* heating AES analysis. For quantification purposes, the measured Auger intensities of the diffusant and the barrier should be normalized by the respective Auger intensities, as recorded from the corresponding pure bulk samples. The surface accumulation parameter [26,51,52] is then defined as:

$$q = \frac{I_A/I_{A\infty}}{I_B/I_{B\infty}}, \tag{9}$$

where I_A and I_B correspond to the measured Auger intensities of the diffusant A and barrier B atoms, respectively; $I_{A\infty}$ and $I_{B\infty}$ are the corresponding A and B intensities for the pure bulk references (serving as experimental Auger sensitivity factors), respectively. Here it is noted that the Auger intensities are typically evaluated from the peak-to-peak heights of derivative AES spectra, since it removes the inelastic electron background intensity.

The surface accumulation parameter q relates to the surface diffusant concentration c_s according to [26,51,52]

$$q = \frac{c_s(1 - \alpha_A^n)}{1 - c_s(1 - \alpha_B^n)} \tag{10}$$

$$\alpha_i = \exp\left(-\frac{1}{\lambda \cos\varphi}\right), \tag{11}$$

where α_i is the so-called attenuation parameter for the solid consisting of atoms of type i = A, B, which includes the inelastic mean free path (IMFP) λ and the emission angle φ of the Auger electrons with respect to the sample surface normal. The parameter n corresponds to the number of diffusant monolayers which have segregated on top of the barrier layer. Note that the amount of monolayers affects the value of δ/δ_s in the parameter S (Eq. (1)) [52]: for one monolayer $\delta/\delta_s \cong 2$; for two monolayers $\delta/\delta_s \cong 1$.

4. Results and discussion

To investigate the influence of stress on the GB diffusion of Cu in W, two types of Cu/W NMLs with different individual Cu and W nanolayers thicknesses were studied: 5 nm Cu / 5 nm W (5Cu/5W) and 10 nm Cu / 3 nm W (10Cu/3W). In both NMLs the repetition ends with a W nanolayer on top. For the analysis of the GB diffusion kinetics, the upper Cu and W nanolayers were considered as source and barrier layers, respectively (Fig. 1). Notably, no intensity from the Cu LMM Auger line could be detected for the as-deposited NMLs (i.e. prior to the annealing), which fulfills an important requirement for selective monitoring of the surface diffusant concentration at the top W barrier nanolayer in time (see Supplementary Information, Part III).

As demonstrated in our previous studies on the thermal stability of Cu/W NMLs [17,22], the Cu and W nanolayers both possess a large compressive residual stress in their as-deposited state, which mainly arises from the high interface stress at the successive Cu/W interfaces. Thermal annealing leads to a gradual relaxation of these stresses, which differs for the Cu and W nanolayers (detailed information on the stress relaxation mechanism can be found in [17,22]). The compressive stresses in the Cu nanolayers are fully relaxed, and the stress state becomes tensile, already after 100 min of annealing in vacuum at 500 °C, which coincides with the appearance of Cu on the surface of the top W nanolayer [17]. On the contrary, substantial compressive stress relaxation in the W nanolayers occurs only towards more elevated temperatures in the range of 700–800 °C (100 min of annealing), which coincides with the degradation of the NML structure [17,22]. Notably, supplementary *in situ* high-temperature stress measurements (see Supplementary Information, P.II) showed that the stress in the W nanolayers remains constant upon cooling down from intermediate annealing temperatures (i.e. 400 °C ≤ T ≤ 600 °C) down to room temperature. This implies that average stress acting on the W barrier nanolayer during thermal annealing can be estimated from the average stress in the W nanolayers, as determined by *ex situ* XRD (after cooling down to room temperature; see Experimental methods).

The stress values derived for the Cu and W nanolayers by XRD represents average in-plane stress values. However, due to the presence of a free surface, the stress level in the top W barrier nanolayer will likely be lower than the averaged W stress level. Besides, probably a stress gradient exists from the bottom to the top of the NML, as successive Cu and W nanolayers can accumulate plastic deformation upon growth. Hence the experimentally determined average stress for all successive W nanolayers in the NML stack should be considered as an upper limit for the stress of the top W barrier nanolayer in contact with the free surface. Previous experimental studies have indicated that the top atomic layers of a thin film can show a stress relaxation of up to 50% at the free surface as compared to the mean film stress [53–55]. Accordingly, as a rough approximation for the model application, the stress in the top W barrier nanolayer was assumed to be 50% smaller than the measured average in-plane stress values of all successive W nanolayers in the NML. The experimentally determined relaxation of the averaged compressive stress of the W nanolayers with increasing annealing time (at constant temperature) approximately follows a linear trend (for both the 5Cu/5W and 10Cu/3W NMLs), as presumed in the applied model according to Eq. (6).

Experimental analysis of the GB diffusion kinetics during annealing on the basis of Eqs. (1) and (7) requires a constant concentration of Cu (diffusant) atoms at the interface between the top W barrier nanolayer and the Cu source nanolayer underneath, i.e. $c_0 = 1$. This requirement (i.e. an infinite Cu source) should be fulfilled, because the ultrafine grain structure of the confined Cu nanolayers provide plenty of short-circuit paths for fast in-plane supply of Cu to the Cu/W interface,

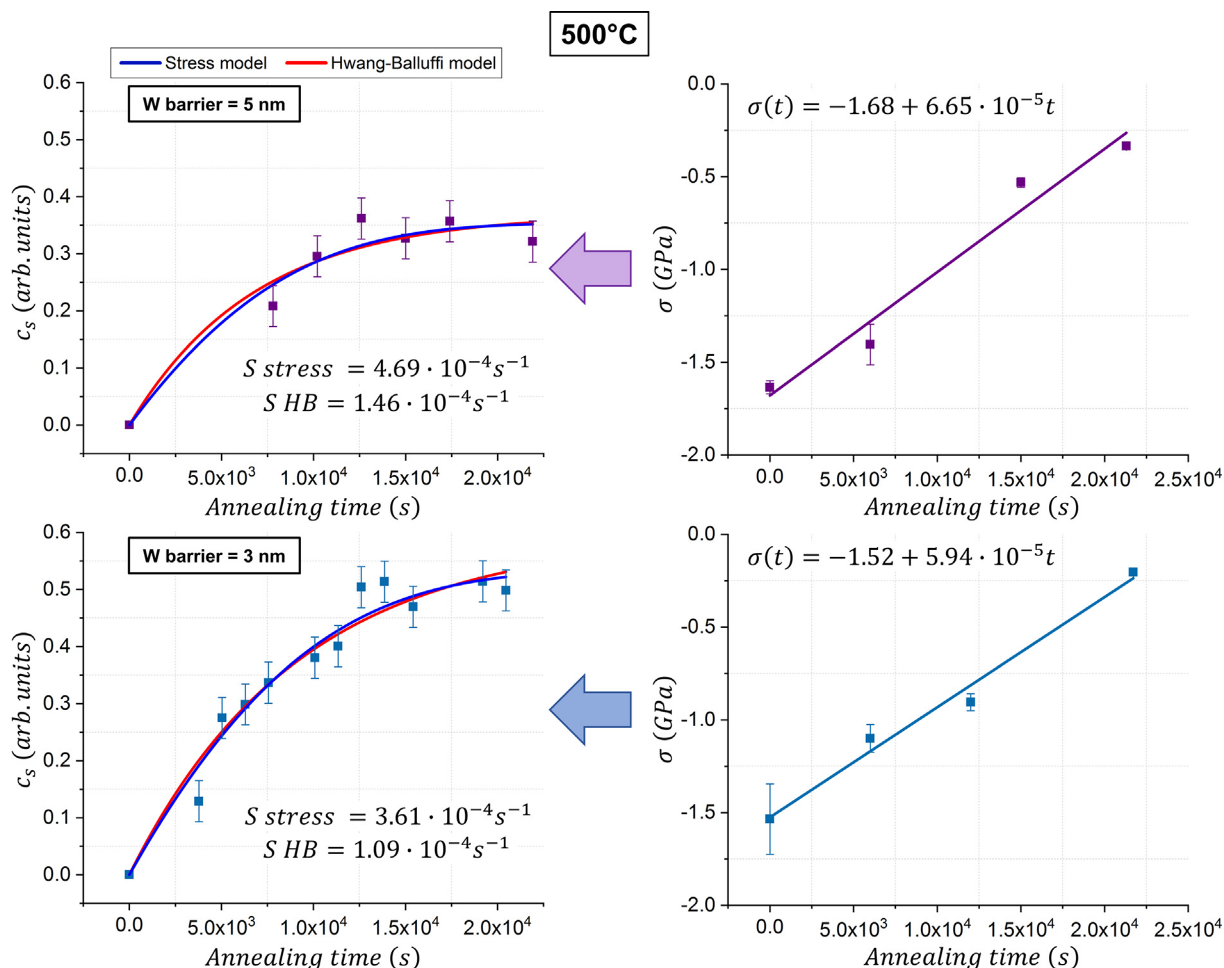

Fig. 3. Cu concentration on the top W barrier nanolayer as function of time, measured by *in situ* AES heating at 500 °C (773 K) for the 5Cu/5W (5 nm W barrier) and 10Cu/3W (3 nm W barrier) NMLs. The values of S were derived by fitting using the Hwang–Balluffi (HB) and Stress models (Eqs. (1) and (7) respectively). The linear functions of $\sigma(t)$ for the Stress model, as determined experimentally by *ex situ* XRD, are shown in the right panels. The error bars for $\sigma(t)$ were derived from the linear fit of the lattice parameter as a function of $\sin^2\psi$, using the CGM method (see Experimental methods). The error bars for $c_s(t)$ were derived from the standard deviation of the Cu surface concentration, as measured *ex situ* at fifteen different locations on the 10Cu/3W NML surface, after annealing at 700 °C for 100 min.

preventing local depletion of Cu during the diffusion process [35]. The compressive stress in the as-deposited Cu nanolayers rapidly decreases during thermal annealing (see above; even becoming slightly tensile stress). Hence it may be assumed that the short-circuit diffusion of Cu atoms in the Cu source nanolayer is not affected by stresses.

The Cu surface concentration on the top W barrier nanolayer of the 5Cu/5W and 10Cu/3W NMLs was monitored by *in situ* AES annealing at constant annealing temperatures of 400 °C, 500 °C and 600 °C. These temperatures are low enough to fulfill the general criterion $T < 0.5T_m^W$ for Type C kinetics, where T_m^W denotes the melting temperature of the W barrier. Although the melting point T_m^W can be depressed at the nanoscale (e.g. $T_m^W = 2673$ °C for 8 nm W nanoparticles [56]), the here applied temperatures are still sufficiently low to maintain Type C kinetics. Reshöft et al. [57] experimentally showed for Cu thin film growth on a W substrate at slightly elevated temperatures that the second Cu monolayer only starts to form after the first Cu monolayer totally covers the W surface. This suggests that the segregation of Cu atoms by grain boundary diffusion on the W surface also spread out on the surface into successive monolayers and the local formation of Cu islands does not occur. In Fig. 3, the measured evolution of the Cu surface concentration, $c_s(t)$, on the top W barrier nanolayer during long-term annealing at 500 °C is presented. The respective concentration curves, $c_s(t)$, of NMLs annealed at 400 °C and 600 °C are shown in the Supplementary Information, P. IV.

For the derivation of $c_s(t)$, the two monolayer limit ($n = 2$) was assumed with $\lambda_{920eVCu_{LMM}} \approx 7$ monolayers, $\lambda_{1736eVW_{MNN}} \approx 8$ monolayers [58] and $\varphi = 45°$ (see Eq. (10)), as proposed by Hwang et al. [26]. The measured saturation levels of $c_s(t)$ are actually less than 1, which implies that the value for n is probably somewhat lower than 2. The k''/k' factor also affects the saturation level [51]. However, the estimates of the number of monolayers n and the associated value of δ/δ_s, will not affect the determination of the activation energy for GB diffusion using Eqs. (1) and (7), since the calculated values of the diffusion coefficients at different temperatures will have the same dependence on δ/δ_s [52], and the effect on the determination of D_0 will thus be negligible.

The classical Hwang–Balluffi model (Eq. (1)), as well as the developed Stress model (Eq. (7)), were fitted to the measured curves of the Cu surface concentration versus time for each annealing temperature introducing the S values and the prefactors, $c_0\frac{k''}{k'}$, as time-independent fit parameters. The thus obtained S values for T = 500 °C are displayed in Fig. 3.

Compared to the Hwang–Balluffi model, the Stress model additionally requires the estimation of the activation volume for diffusion Ω. A diffusion activation volume of $0.8V_m$ was found experimentally for the GB diffusion of Zn in Al, where V_m is the molar volume of Al [59]. Due to the absence of experimental data for the GB diffusion in W, the activation volume for Cu GB diffusion in W was also assumed as $0.8V_m^W$ with $V_m^W \approx 7.69 \cdot 10^{-6} \frac{m^3}{mol}$ [60].

Provided that no significant microstructural changes of the diffusion

barrier occur during annealing (i.e. the GB structure, surface structure and grain size remain stable), the values of the GB width (δ), the thickness of the segregated surface film (δ_s) and the average columnar grain size (d) can be taken as a constant for all annealing times and temperatures studied. As shown in our previous work [22], thermal grooving of W GBs with concurrent W grain coarsening in Cu/W NMLs only starts after prolonged annealing, while complete W stress relaxation only takes place at more elevated temperatures (T > 700 °C). Although some stress relaxation can occur during the *in situ* heating AES study, a significant stress relaxation in the W nanolayers (also in the top W barrier nanolayer) can be excluded for the studied moderate annealing temperatures and times. Moreover, the in-plane and out-of-plane texture in the as-deposited 5Cu/5W and 10Cu/3W NMLs (according to Cu{1 1 1} < −1 0 1 > ||W{1 1 0} < −1 1 1 >) is conserved upon annealing up to 700 °C [22], which suggests that the GB network of the as-deposited W barrier layers is largely preserved in the current study. Finally, the local equilibria at the junction of the GB with the free surface and at the junction of the GB with the source layer, as defined by the segregation coefficients $k^{''}$ and $k^{'}$, can also be taken constant (although, these local equilibria may show some temperature dependence [51]).

Based on the above assumptions, the activation energy for GB diffusion can be estimated from the experimentally derived S values at each temperature through an Arrhenius analysis. Fig. 4(a,b) show a corresponding Arrhenius analysis for the 10Cu/3W and 5Cu/5W NMLs and also reports the extracted activation energies for GB diffusion of Cu in W. This results in estimated activation energies for Cu diffusion along W GBs of ~0.45 eV for the Hwang–Balluffi model and of ~0.29 eV for the Stress model. This indicates that the presence of high internal stresses in the W barrier nanolayer increases the effective activation energy for Cu diffusion in W GBs by a factor of about 1.5. Thus, high compressive stresses in the W barrier nanolayer considerably slow down the kinetics of Cu diffusion in W GBs.

In Fig. 4(c), the derived activation energies (E_A and E_A^*) are compared to reported literature values, as obtained for other metallic systems using the Hwang–Balluffi model. The estimated activation energies of 0.45 eV and 0.29 eV, as determined for Cu GB diffusion in W, fall well within the very broad range of reported activation energies for GB diffusion in other metallic bilayer systems (i.e. from about 0.1 eV to 1.0 eV). Notably, the reported activation energies do not consider the effect of internal stresses in the diffusion barrier on the GB diffusion kinetics.

For the sputter-deposition of metallic layers with a thickness of several nanometers, the columnar width of the grains roughly equals on the order of the layer thickness: i.e. $h \cong d$. In this case, the diffusion coefficients can be estimated from the experimentally derived S parameters, assuming $k^{''} \cong 1$ for the two monolayer limit $\delta/\delta_s \cong 1$. The difference between the derived diffusion coefficients for the 5Cu/5W and 10Cu/3W NMLs is within the experimental error of the AES *in situ* analysis. The average GB diffusion coefficients of Cu in W for the stress-free state of the W barrier nanolayer at different annealing temperatures are given in Table 1. The corresponding pre-exponential factor of the GB diffusion coefficient (Eqs. (5) and (3)) is $D_0 = (3.2 \pm 0.6) \times 10^{-15}$ cm²/s (error is calculated from the least squares fitting in the $\ln(D_b^*)(1/T)$ logarithmic plot).

The main thermodynamic driving force for the NML-to-NC transition arises from the minimization of the excess Gibbs energies associated with the reduction of internal interfaces (Cu/Cu and W/W GBs

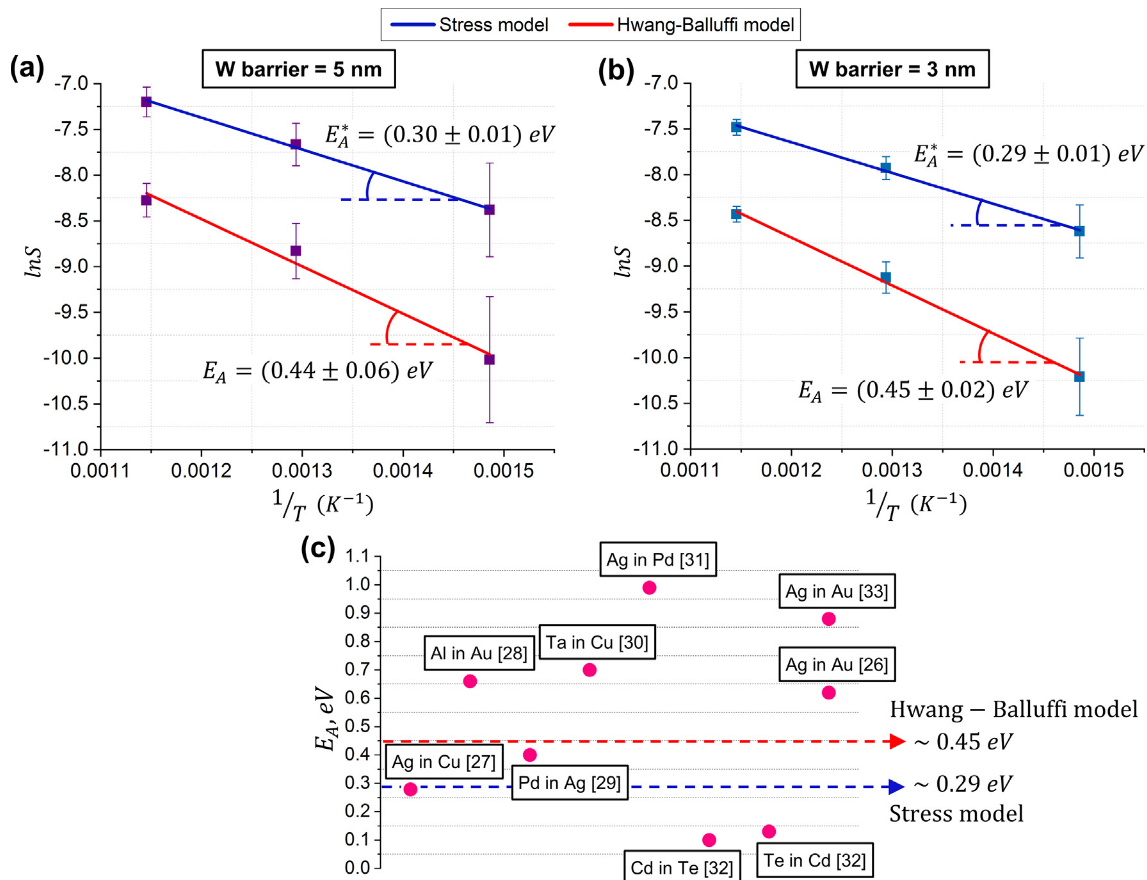

Fig. 4. Experimentally determined activation energies of Cu GB diffusion in W by application of the Hwang–Balluffi and Stress models. (a) and (b) Arrhenius analysis of S parameters for the 5Cu/5W and 10Cu/3W NMLs, respectively. (c) Comparison of the estimated activation energies from the present study with activation energies reported for other metallic systems (bilayer thin films, as experimentally derived using the Hwang–Balluffi model for type C kinetics). Error bars for the S values were derived from the fit of $c_s(t)$. The error for the activation energy is calculated from the least squares fit in Arrhenius plot.

Table 1
The average GB diffusion coefficients of Cu in W for a stress-free state of the W barrier nanolayer at different temperatures.

T(K)	Stress-free Cu GB diffusion coefficients in W D_b^* (cm^2/s)
673	$(1.8 \pm 1.1) \times 10^{-17}$
773	$(3.7 \pm 0.9) \times 10^{-17}$
873	$(5.9 \pm 0.9) \times 10^{-17}$

and Cu/W interfaces) and the relaxation of internal stresses [14,17]. The initial stage of the NML-to-NC transition in Cu/W NMLs, investigated here by *in situ* heating AES analysis, proceeds by the diffusion of Cu atoms though the GBs to the surface of the top W barrier nanolayer. As a result, (high-angle) W GBs may become wetted by Cu striving to reduce the GB energy. Also the segregation and diffusion of Cu on the surface of the top W barrier will be associated by a reduction of the surface energy. Notably, the *in situ* heating AES analysis showed that the Cu surface concentration saturates with time, which implies that the driving forces for GB wetting and surface segregation only contribute to the initial stage of the NML-to-NC transition. Subsequent reduction of excess Gibbs energies associated with the internal interfaces will require thermally activated diffusion of W at more elevated temperatures. As such, thermal grooving of the W GBs can proceed, which eventually leads to a pinching-off of the nanolayers, and a spheroidization of the microstructure to form a NC [14,17].

5. Conclusions

The diffusion of Cu across W GBs upon annealing of sputter-deposited Cu/W NMLs was investigated by *in-situ* heating AES and *ex-situ* XRD, accounting for the effect of compressive stresses in the W barrier layers on the Cu GB diffusion kinetics. The stress-free activation energies and diffusion coefficient for Cu diffusion along W GBs could be determined by fitting the measured course of the surface concentration of Cu during the annealing to the predicted concentration profiles, as calculated using a modified diffusion model that accounts for stress relaxation in the W barrier nanolayer during the annealing

The stress-free activation energy of 0.29 eV for Cu diffusion in W GBs was found to be considerably lower than the respective value of 0.45 eV, as determined by Hwang–Balluffi without accounting for the effect of compressive stresses in the W barrier nanolayer on the Cu GB diffusion kinetics. This analysis shows that the stress state of the diffusion barrier layer can have a pronounced effect on the GB diffusion kinetics and therefore needs to be accounted for studying diffusion-controlled phase and/or microstructure transformation kinetics in nanocrystalline materials and nanoscale thin films.

The stress-free Cu GB diffusion coefficient in W, as derived in this study, is of particular importance for predicting the thermal stability of Cu/W NMLs during annealing and, more specifically, for controlling the kinetics of the NML-to-NC transformation. The reported diffusion model can generally be employed to nanoscale thin films and NMLs of various material systems, where the mean stress evolution with time follows a linear dependence.

Declaration of Competing Interest

The authors declare that they have no known competing financial interests or personal relationships that could have appeared to influence the work reported in this paper.

Acknowledgement

The authors thank Dr. X. Maeder at Empa Thun, for his valuable support in the in situ high-temperature stress measurements. The authors are also grateful to Dr. R. Hauert for technical support and help in the Auger experiments. This work was funded by the EU FP7-PEOPLE-2013-IRSES Project EXMONAN- Experimental investigation and modelling of nanoscale solid state reactions with high technological impact (Grant No. 612552); by RFBR, project number 19-33-90125; by NUST "MISIS" scholarship for studying abroad and by Ministry of Education and Science of the Russian Federation in the framework of the Program to Increase the Competitiveness of NUST "MISIS" as well as state task.

Appendix A. Supplementary material

Supplementary data to this article can be found online at https://doi.org/10.1016/j.apsusc.2020.145254.

References

[1] D. Raabe, M. Herbig, S. Sandlöbes, Y. Li, D. Tytko, M. Kuzmina, D. Ponge, P.-P. Choi, Grain boundary segregation engineering in metallic alloys: a pathway to the design of interfaces, Curr. Opin. Solid State Mater. Sci. 18 (2014) 253–261, https://doi.org/10.1016/j.cossms.2014.06.002.

[2] A. Misra, R.G. Hoagland, H. Kung, Thermal stability of self-supported nanolayered Cu/Nb films, Philos. Mag. 84 (2004) 1021–1028, https://doi.org/10.1080/14786430310001659480.

[3] D. Josell, F. Spaepen, Surfaces, interfaces, and changing shapes in multilayered films, MRS Bull. 24 (1999) 39–43, https://doi.org/10.1557/S0883769400051538.

[4] B.Y. Zhang, B.X. Liu, J.N. He, W. Fang, F.Y. Zhang, X. Zhang, C.X. Chen, F.X. Yin, Microstructure and mechanical properties of SUS304/Q235 multilayer steels fabricated by roll bonding and annealing, Mater. Sci. Eng. A. 740–741 (2019) 92–107, https://doi.org/10.1016/j.msea.2018.10.054.

[5] W.X. Yu, B.X. Liu, J.N. He, C.X. Chen, W. Fang, F.X. Yin, Microstructure characteristics, strengthening and toughening mechanism of rolled and aged multilayer TWIP/maraging steels, Mater. Sci. Eng. A. 767 (2019) 138426, , https://doi.org/10.1016/j.msea.2019.138426.

[6] C. Huber, H. Sepehri-Amin, M. Goertler, M. Groenefeld, I. Teliban, K. Hono, D. Suess, Coercivity enhancement of selective laser sintered NdFeB magnets by grain boundary infiltration, Acta Mater. 172 (2019) 66–71, https://doi.org/10.1016/j.actamat.2019.04.037.

[7] W. Cui, T. Zhang, X. Zhou, D. Yu, Q. Wang, X. Zhao, W. Liu, Z. Zhang, Enhanced coercivity and grain boundary chemistry in diffusion-processed Ce13Fe79B8 ribbons, Mater. Lett. 191 (2017) 210–213, https://doi.org/10.1016/j.matlet.2016.12.060.

[8] H. Li, X. Su, X. Tang, Q. Zhang, C. Uher, G.J. Snyder, U. Aydemir, Grain boundary engineering with nano-scale InSb producing high performance In x Ce y Co 4 Sb 12+z skutterudite thermoelectrics, J. Mater. 3 (2017) 273–279, https://doi.org/10.1016/j.jmat.2017.07.003.

[9] K.T. Nam, A. Datta, S.-H. Kim, K.-B. Kim, Improved diffusion barrier by stuffing the grain boundaries of TiN with a thin Al interlayer for Cu metallization, Appl. Phys. Lett. 79 (2001) 2549–2551, https://doi.org/10.1063/1.1409594.

[10] S.-H. Kim, K.T. Nam, A. Datta, H.-M. Kim, K.-B. Kim, D.-H. Kang, Multilayer diffusion barrier for copper metallization using a thin interlayer metal (M = Ru, Cr, and Zr) between two TiN films, J. Vac. Sci. Technol. B Microelectron. Nanom. Struct. 21 (2003) 804, https://doi.org/10.1116/1.1562645.

[11] D. Josell, J.E. Bonevich, T.M. Nguyen, R.N. Johnson, Heat transfer through nanoscale multilayered thermal barrier coatings at elevated temperatures, Surf. Coatings Technol. 275 (2015) 75–83, https://doi.org/10.1016/j.surfcoat.2015.05.036.

[12] A. Tiwari, M.K. Tiwari, M. Gupta, H.-C. Wille, A. Gupta, Interface sharpening in miscible and isotopic multilayers: role of short-circuit diffusion, Phys. Rev. B. 99 (2019) 205413, , https://doi.org/10.1103/PhysRevB.99.205413.

[13] A. Maesaka, N. Sugawara, A. Okabe, M. Itabashi, Influence of microstructure on thermal stability of spin-valve multilayers, J. Appl. Phys. 83 (1998) 7628–7634, https://doi.org/10.1063/1.367880.

[14] F. Moszner, C. Cancellieri, M. Chiodi, S. Yoon, D. Ariosa, J. Janczak-Rusch, L.P.H. Jeurgens, Thermal stability of Cu/W nano-multilayers, Acta Mater. 107 (2016) 345–353, https://doi.org/10.1016/j.actamat.2016.02.003.

[15] M. Hecker, J. Thomas, D. Tietjen, S. Baunack, C.M. Schneider, A. Qiu, N. Cramer, R.E. Camley, Z. Celinski, Thermally induced modification of GMR in Co/Cu multilayers: correlation among structural, transport, and magnetic properties, J. Phys. D. Appl. Phys. 36 (2003) 564–572, https://doi.org/10.1088/0022-3727/36/5/322.

[16] P. Troche, J. Hoffmann, K. Heinemann, F. Hartung, G. Schmitz, H.C. Freyhardt, D. Rudolph, J. Thieme, P. Guttmann, Thermally driven shape instabilities of Nb/Cu multilayer structures: instability of Nb/Cu multilayers, Thin Solid Films 353 (1999) 33–39, https://doi.org/10.1016/S0040-6090(99)00365-X.

[17] A.V. Druzhinin, D. Ariosa, S. Siol, N. Ott, B.B. Straumal, J. Janczak-Rusch, L.P.H. Jeurgens, C. Cancellieri, Effect of the individual layer thickness on the transformation of Cu/W nano-multilayers into nanocomposites, Materialia 7 (2019) 100400, , https://doi.org/10.1016/j.mtla.2019.100400.

[18] W.M. Daoush, J. Yao, M. Shamma, K. Morsi, Ultra-rapid processing of high-hardness tungsten–copper nanocomposites, Scr. Mater. 113 (2016) 246–249, https://doi.org/10.1016/J.SCRIPTAMAT.2015.11.012.

[19] A. Fathy, O. El-Kady, Thermal expansion and thermal conductivity characteristics of Cu–Al2O3 nanocomposites, Mater. Des. 46 (2013) 355–359, https://doi.org/10.

1016/j.matdes.2012.10.042.

[20] S. Pan, M. Sokoluk, C. Cao, Z. Guan, X. Li, Facile fabrication and enhanced properties of Cu-40 wt% Zn/WC nanocomposite, J. Alloys Compd. 784 (2019) 237–243, https://doi.org/10.1016/j.jallcom.2019.01.022.

[21] Z. Wang, L. Gu, F. Phillipp, J.Y. Wang, L.P.H. Jeurgens, E.J. Mittemeijer, Metal-catalyzed growth of semiconductor nanostructures without solubility and diffusivity constraints, Adv. Mater. 23 (2011) 854–859, https://doi.org/10.1002/adma.201002997.

[22] C. Cancellieri, F. Moszner, M. Chiodi, S. Yoon, J. Janczak-Rusch, L.P.H. Jeurgens, The effect of thermal treatment on the stress state and evolving microstructure of Cu/W nano-multilayers, J. Appl. Phys. 120 (2016) 195107, , https://doi.org/10.1063/1.4967992.

[23] A.S. Ostrovsky, B.S. Bokstein, Grain boundary diffusion in thin films under stress fields, Appl. Surf. Sci. 175–176 (2001) 312–318, https://doi.org/10.1016/S0169-4332(01)00164-7.

[24] A. Ostrovsky, Grain boundary diffusion in thin films under stress field in kinetic regime “C”, Defect Diffus. Forum. 156 (1998) 249–254, https://doi.org/10.4028/www.scientific.net/DDF.156.249.

[25] N. Balandina, B.S. Bokstein, A. Ostrovsky, Copper diffusion in nickel thin film under stresses in the kinetic regime “B”, Defect Diffus. Forum. 156 (1998) 181–190, https://doi.org/10.4028/www.scientific.net/DDF.156.181.

[26] J.C.M. Hwang, J.D. Pan, R.W. Balluffi, Measurement of grain-boundary diffusion at low temperature by the surface-accumulation method. II. Results for gold-silver system, J. Appl. Phys. 50 (1979) 1349–1359, https://doi.org/10.1063/1.326115.

[27] J.M. Schoen, J.M. Poate, C.J. Doherty, C.M. Melliar-Smith, Grain-boundary diffusion of Ag through Cu films, J. Appl. Phys. 50 (1979) 6910–6914, https://doi.org/10.1063/1.325842.

[28] Z. Bastl, J. Židů, K. Roháček, Determination of the diffusion coefficient of aluminum along the grain boundaries of gold films by the surface accumulation method, Thin Solid Films 213 (1992) 103–108, https://doi.org/10.1016/0040-6090(92)90482-Q.

[29] G. Balcerowska, A. Bukaluk, R. Siuda, J. Seweryn, M. Rozwadowski, Grain boundary diffusion of Pd through Ag thin layers evaporated on polycrystalline Pd in high vacuum studied by means of AES, PCA and FA, Vacuum 54 (1999) 93–97, https://doi.org/10.1016/S0042-207X(98)00442-4.

[30] G. Erdélyi, G. Langer, J. Nyéki, L. Kövér, C. Tomastik, W.S.M. Werner, A. Csik, H. Stoeri, D.L. Beke, Investigation of Ta grain boundary diffusion in copper by means of Auger electron spectroscopy, Thin Solid Films 459 (2004) 303–307, https://doi.org/10.1016/j.tsf.2003.12.125.

[31] Z. Balogh, Z. Erdélyi, D.L. Beke, A. Portavoce, C. Girardeaux, J. Bernardini, A. Rolland, Silver grain boundary diffusion in Pd, Appl. Surf. Sci. 255 (2009) 4844–4847, https://doi.org/10.1016/j.apsusc.2008.12.010.

[32] A. Jadin, R. Andrew, M. Wautelet, B. Dumont, L.D. Laude, Grain boundary interdiffusion in Cd/Te thin film couples, Thin Solid Films 148 (1987) 163–169, https://doi.org/10.1016/0040-6090(87)90154-4.

[33] A. Bukaluk, Determination of the activation energy of Ag diffusion through grain boundaries of thin Au films by using AES in a simplified accumulation method, Appl. Surf. Sci. 35 (1989) 317–326, https://doi.org/10.1016/0169-4332(89)90015-9.

[34] G.L. Harrison, Influence of dislocations on kinetics in solids with particular reference to the alkali halides, Trans. Faraday Soc. 57 (1961) 1191–1199, https://doi.org/10.1039/tf9615701191.

[35] J.C.M. Hwang, R.W. Balluffi, Measurement of grain-boundary diffusion at low temperatures by the surface accumulation method. I. Method and analysis, J. Appl. Phys. 50 (1979) 1339–1348, https://doi.org/10.1063/1.326168.

[36] C.A. Friskney, C.W. Haworth, Heat-flow problems in electron-probe microanalysis, J. Appl. Phys. 38 (1967) 3796–3798, https://doi.org/10.1063/1.1710222.

[37] S. Hofmann, A. Zalar, Electron beam effects during the sputter profiling of thin Au/Ag films analysed by Auger electron spectroscopy, Thin Solid Films 56 (1979) 337–342, https://doi.org/10.1016/0040-6090(79)90135-4.

[38] B.M. Clemens, J.A. Bain, Stress determination in textured thin films using X-ray diffraction, MRS Bull. 17 (1992) 46–51, https://doi.org/10.1557/S0883769400041658.

[39] M. Birkholz, Thin Film Analysis by X-Ray Scattering, Wiley-VCH Verlag GmbH & Co. KGaA, Weinheim, FRG, 2005, https://doi.org/10.1002/3527607595.

[40] H.M. Otte, Lattice parameter determinations with an X-ray spectrogoniometer by the Debye-Scherrer method and the effect of specimen condition, J. Appl. Phys. 32 (1961) 1536–1546, https://doi.org/10.1063/1.1728392.

[41] W. Parrish, Results of the IUCr precision lattice-parameter project, Acta Crystallogr. 13 (1960) 838–850, https://doi.org/10.1107/S0365110X60002041.

[42] W.C. Overton, J. Gaffney, Temperature variation of the elastic constants of cubic elements. I. Copper, Phys. Rev. 98 (1955) 969–977, https://doi.org/10.1103/PhysRev.98.969.

[43] F.H. Featherston, J.R. Neighbours, Elastic constants of tantalum, tungsten, and molybdenum, Phys. Rev. 130 (1963) 1324–1333, https://doi.org/10.1103/PhysRev. 130.1324.

[44] A.S. Ostrovsky, N. Balandina, B.S. Bokstein, Models for grain boundary diffusion in thin films under stress fields in different kinetic regimes, Mater. Sci. Forum. 294–296 (1998) 553–556, https://doi.org/10.4028/www.scientific.net/MSF.294-296.553.

[45] R.C. Cammarata, Surface and interface stress effects in thin films, Prog. Surf. Sci. 46 (1994) 1–38, https://doi.org/10.1016/0079-6816(94)90005-1.

[46] R.C. Cammarata, K. Sieradzki, F. Spaepen, Simple model for interface stresses with application to misfit dislocation generation in epitaxial thin films, J. Appl. Phys. 87 (2000) 1227–1234, https://doi.org/10.1063/1.372001.

[47] T.H. Courtney, Mechanical Behavior of Materials, second ed., McGraw Hill, Boston, 2000.

[48] C. Cancellieri, E. Klyatskina, M. Chiodi, J. Janczak-Rusch, L.P.H. Jeurgens, The effect of interfacial Ge and RF-bias on the microstructure and stress evolution upon annealing of Ag/AlN multilayers, Appl. Sci. 8 (2018) 2403, https://doi.org/10.3390/app8122403.

[49] D.G. Liu, L. Zheng, J.Q. Liu, L.M. Luo, Y.C. Wu, Residual stress relief of hard a-C films though buckling, Ceram. Int. 44 (2018) 3644–3648, https://doi.org/10.1016/j.ceramint.2017.11.115.

[50] X. Chen, X. Pang, J. Meng, H. Yang, Thermal-induced blister cracking behavior of annealed sandwich-structured TiN/CrAlN films, Ceram. Int. 44 (2018) 5874–5879, https://doi.org/10.1016/j.ceramint.2017.12.014.

[51] Z. Erdélyi, C. Girardeaux, G.A. Langer, D.L. Beke, A. Rolland, J. Bernardini, Determination of grain-boundary diffusion of Ag in nanocrystalline Cu by the Hwang-Balluffi method, J. Appl. Phys. 89 (2001) 3971–3975, https://doi.org/10.1063/1.1346658.

[52] Z. Erdélyi, C. Girardeaux, G.A. Langer, L. Daróczi, A. Rolland, D.L. Beke, Determination of grain-boundary diffusion coefficients by Auger electron spectroscopy, Appl. Surf. Sci. 162 (2000) 213–218, https://doi.org/10.1016/S0169-4332(00)00194-X.

[53] M.F. Doerner, S. Brennan, Strain distribution in thin aluminum films using x-ray depth profiling, J. Appl. Phys. 63 (1988) 126–131, https://doi.org/10.1063/1.340503.

[54] R. Treml, D. Kozic, J. Zechner, X. Maeder, B. Sartory, H.-P. Gänser, R. Schöngrundner, J. Michler, R. Brunner, D. Kiener, High resolution determination of local residual stress gradients in single- and multilayer thin film systems, Acta Mater. 103 (2016) 616–623, https://doi.org/10.1016/j.actamat.2015.10.044.

[55] J. Keckes, R. Daniel, J. Todt, J. Zalesak, B. Sartory, S. Braun, J. Gluch, M. Rosenthal, M. Burghammer, C. Mitterer, S. Niese, A. Kubec, 30 nm X-ray focusing correlates oscillatory stress, texture and structural defect gradients across multilayered TiN-SiOx thin film, Acta Mater. 144 (2018) 862–873, https://doi.org/10.1016/j.actamat.2017.11.049.

[56] A. Moitra, S. Kim, J. Houze, B. Jelinek, S.-G. Kim, S.-J. Park, R.M. German, M.F. Horstemeyer, Melting tungsten nanoparticles: a molecular dynamics study, J. Phys. D. Appl. Phys. 41 (2008) 185406, , https://doi.org/10.1088/0022-3727/41/18/185406.

[57] K. Reshöft, C. Jensen, U. Köhler, Atomistics of the epitaxial growth of Cu on W (110), Surf. Sci. 421 (1999) 320–336, https://doi.org/10.1016/S0039-6028(98)00859-0.

[58] C.J. Powell, A. Jablonski, NIST Electron Inelastic-Mean-Free-Path Database, Version 1, National Institute of Standards and Technology, Gaithersburg, MD, 2010.

[59] G. Erdélyi, W. Łojkowski, D.L. Beke, I. Gödény, F.J. Kedeves, The pressure dependence of grain-boundary diffusion of 65 Zn in polycrystalline aluminium, Philos. Mag. A. 56 (1987) 673–680, https://doi.org/10.1080/01418618708204480.

[60] L.S. Dubrovinsky, S.K. Saxena, Thermal expansion of periclase (MgO) and tungsten (W) to melting temperatures, Phys. Chem. Miner. 24 (1997) 547–550, https://doi.org/10.1007/s002690050070.